THESIS FOR THE DEGREE OF DOCTOR OF PHILOSOPHY

GNSS Signal Diffraction Effects in High Precision Positioning

UTTAMA DUTTA

Department of Physics and Astronomy - Onsala Space Observatory
CHALMERS UNIVERSITY OF TECHNOLOGY
Gothenburg, Sweden, 2026

GNSS Signal Diffraction Effects in High Precision Positioning

Uttama Dutta
ISBN 978-91-8103-461-5

Acknowledgements, dedications, and similar personal statements in this thesis, reflect the author's own views.

Selected material from the author's licentiate thesis: Uttama Dutta, "Enhancing the reliability of GNSS carrier phase measurements for precise positioning applications", *Chalmers Tekniska Hogskola*, Gothenburg, Sweden, August 2024, is republished in this Ph.D. thesis.

Doktorsavhandlingar vid Chalmers tekniska högskola
Ny serie nr 5918
ISSN 0346-718X

Department of Physics and Astronomy - Onsala Space Observatory
Chalmers University of Technology
SE-412 96 Gothenburg, Sweden
Phone: +46 (0)31 772 1000

Printed by Chalmers Digital Printing
Gothenburg, Sweden, August 2026

GNSS Signal Diffraction Effects in High Precision Positioning

UTTAMA DUTTA
Department of Physics and Astronomy - Onsala Space Observatory
Chalmers University of Technology

Abstract

High-precision GNSS is fundamental to modern geodesy. Standard processing assumes line-of-sight signal propagation, treating residual non-line-of-sight effects as multipath or random noise. This thesis shows that diffraction caused by signal bending around obstacles, is a distinct, deterministic error source that biases key geodetic parameters (coordinates, troposphere) in ways that averaging or double-differencing cannot remove.

Unmodeled diffraction introduces slowly varying carrier-phase biases that affect station coordinates (especially the vertical component), hinder ambiguity resolution, and mimic tropospheric zenith delays. Under common field conditions (e.g., a 1 m obstacle at 1 m distance), biases can reach decimeter levels, leading to false interpretations of tectonic motion, seasonal deformation, or local subsidence. Because diffraction correlates with satellite geometry, it aliases into tropospheric estimates, degrading climate-related GNSS applications. The DOP metric alone is insufficient, and conventional multipath mitigation (choke rings, absorbers) is largely ineffective against diffraction.

This thesis makes four novel contributions. First, it clearly distinguishes diffraction from multipath using GNSS SNR observables and carrier-phase residuals (from PPP and double differences), resolving a long-standing ambiguity. Second, a controlled movable-wall experiment quantifies the inverse distance dependence of diffraction error, validates knife-edge models at far-field (2 m) while revealing their near-field limitations (1 m), and derives an operational guideline (obstacle subtended angle $<11^\circ$) for PPP and RTK. Third, a first-of-its-kind phasor-based, data-driven interference model for near-field cylindrical interference achieves correlations >0.61 and mm-level residuals, turning empirical site-calibration maps into interpretable physical models. Fourth, diffraction analysis is extended to tropospheric parameter estimation, uncovering previously undocumented errors in estimated zenith total delays and gradients.

The thesis includes three introductory chapters (GNSS error sources, diffraction theory, post-processing software) and five appended papers. Together, they reclassify diffraction from a neglected phenomenon into a quantifiable, modelable one, with direct implications for monument design, site selection, and interpretation of long-term coordinate time series in high-precision geodesy.

Keywords: GNSS, Diffraction, High-precision positioning, Carrier phase, Multipath, NLOS, PPP, RTK, SNR, Fresnel zone.

List of Publications

This thesis is based on the following publications:

[A] **Uttama Dutta**, Jan Johansson, Rüdiger Haas, "Investigating the impact of diffraction on GNSS carrier phase measurements". *Journal of Geodesy*, vol. 100, no. 4, SP 25, April 2026.
This document is the 'Accepted Manuscript' version. The 'Version of Record' of this article is available online at:
https://doi.org/10.1007/s00190-026-02045-w

[B] **Uttama Dutta**, Jan M. Johansson, Rüdiger Haas, Sten E.G. Bergstrand, Carsten Rieck, "Experimental Characterization of GNSS Carrier Phase Diffraction Errors in a Controlled Environment". *GPS Solutions. in review*

[C] **Uttama Dutta**, Jan M. Johansson, "Study of GNSS Phase Center Perturbations from Cylindrical Obstructions". *Journal of Geodesy. in review*

[D] **Uttama Dutta**, Jan Johansson, "Multi-Constellation/Multi-Frequency GNSS Signal Degradation Due to Foliage and Reflective Environments". *Engineering Proceedings*, vol. 54, no. 1, p. 2, Sep. 2023.
https://doi.org/10.3390/ENC2023-15454

[E] **Uttama Dutta**, Jan M. Johansson, Peng Feng, "Impact of Diffraction on GNSS Troposphere Estimates in a Controlled Environment". *Manuscript to be submitted*

Other publications by the author, not included in this thesis, are:

[1] **Uttama Dutta**, Carsten Rieck, Martin Håkansson, Daniel Gerbeth, Samieh Alissa, Stefan Nord, "Satellite Selection in the Context of Network RTK for Limited Bandwidth Applications". *Proceedings of the 34th International Technical Meeting of the Satellite Division of The Institute of Navigation (ION GNSS+ 2021)* , 2474 - 2492, https://doi.org/10.33012/2021.17948.

[2] **Uttama Dutta**, Per Jarlemark, Carsten Rieck, Jan Johansson, "Ionospheric Effects on GNSS RTK". *Proceedings of the 35th International Technical Meeting of the Satellite Division of The Institute of Navigation (ION GNSS+ 2022)* , 1589-1598, https://doi.org/10.33012/2022.18297 .

[3] Samieh Alissa, Martin Håkansson, Carsten Rieck, **Uttama Dutta**, Stefan Nord, Peter Bergljung, Anders Bagge, "Distribution of the Adapted-NRTK

Correction Data via VDES for the Shipping Navigation Safety". *Proceedings of the 34th International Technical Meeting of the Satellite Division of The Institute of Navigation (ION GNSS+ 2021)* , 521 - 534, https://doi.org/10.33012/2021.18142.

Contents

Acknowledgments

Like every PhD journey, mine too came with disturbances which are sometimes quite overpowering, and you find the real signal (the original motivation) drowning in the noise floor (the disturbances). But the key is to 'stay afloat' long enough. While the noise is ever present, you eventually develop an adaptive noise cancellation filter that is finally ready to pull out the real signal even in the worst of adversities. I am full of gratitude to all who helped me stay afloat.

I would first like to thank my supervisor, Prof. Jan M. Johansson, an ideal teacher. Even after a long and tiring day, he remained calm and patient, offering insightful suggestions and encouraging words. He taught me to be relentless and systematic in verifying every detail in my pursuit of correct results. I also thank my supervisor Prof. Rüdiger Haas for all his wonderful support and encouragement and for showing me how to stay focused on only what is important. A special thanks to my examiner Prof. Lars Ulander for his unbiased advices at times when I needed them the most. Thank you Prof. Vincent Desmaris for your help with the popular science presentation. I am thankful to Lantmäteriet for providing the required infrastructure.

I would like to thank RISE Research Institutes of Sweden for the financial support. A big thanks to Martin Bjerling, Jörgen Spetz, Sten Bergstrand, Carsten Rieck and all the wonderful colleagues of my unit 'Dimension and Position'.

A big shout out to the Technical Support Group (TSG) at the Onsala Space Observatory, especially Roger Hammargren, Magnus Kjerling and Rolf Ahlman. Without you, my 'crazy' experiments in the extreme weather conditions would have been impossible. My colleagues at Chalmers, especially Rimsky and Alva, created a nice work environment and thanks to you, I am going to cherish happy memories of my life at Chalmers. Thank you Peng and Alva for making the observatory more accessible.

I have always enjoyed the 'PhD discussion' meetings meant for discussing research alone (the fun part), and I am thankful to Jan, Rüdiger, Carsten, Sten and Peng for joining these actively. It is a missed opportunity for me to not have had the late Per Jarlemark in one of these meetings, but nevertheless I am thankful to him for leaving a legacy of great research behind.

On a more personal note, they say that there is a woman behind every successful man. But do they know that behind a successful woman, there is usually a loving family? A husband, who would go to any lengths to support the wife, a loving and caring mother, a brother full of wisdom, an extremely patient daughter and last but not the least a father that believed. When you find love and support that is unquestionable, you are bound to remain afloat even in the worst of tides. Thank you for being there!

"Knowledge is empowering. But arrogance is a kind of amnesia. The cure is remembering – not once, but daily – the true scale of things. Sagan's pale blue dot suspended in an ocean of darkness, is home to everyone who ever thought themselves a giant. Grasp that smallness, and the urge to diminish others quietly heals." - Anonymous

Acronyms

GNSS:	Global Navigation Satellite Systems
NLOS:	Non Line of Sight.
LOS:	Line of Sight.
SGP:	Shortest Geometric Path
PPP:	Precise Point Positioning
RTK:	Real Time Kinematic
SNR:	Signal-to-noise ratio
DOP:	Dilution of Precision
ZTD:	Zenith Total Delay
KED:	Knife Edge Diffraction
PDP:	Power Delay Profile
MDR:	Multipath to direct signal ratio

Part I

Overview

CHAPTER 1

Introduction and Motivation

High-precision Global Navigation Satellite System (GNSS) positioning, rests on a seemingly simple assumption, that the signal received from a satellite traveled along a straight, unobstructed line-of-sight path. Yet, real-world GNSS antennas are rarely installed in ideal environments. Vegetation, buildings, walls, poles, and even the antenna mount itself can intrude into the signal's propagation path. When such intrusion occurs, the signal does not simply disappear but rather diffracts. This physical process bends the electromagnetic wave around the obstacle's edge, creating an erroneous measurement that still appears valid to standard geodetic processing software. The resulting error is systematic, structured, and persistent. It degrades coordinate solutions and biases derived parameters such as tropospheric zenith delays. Unlike more familiar error sources, diffraction cannot be averaged out, nor is it eliminated by double-differencing. This thesis provides a comprehensive investigation of diffraction from a geodetic perspective, combining theoretical development, controlled experimentation, and advanced modeling to characterize its signatures, distinguish it from multipath, and quantify its impact on millimeter-level GNSS applications.

1.1 Significance of GNSS errors

Since diffraction is not the only error source, let us first take a close look at the various GNSS error sources. The two principal measurement types used for positioning are code-based pseudoranges and carrier-phase measurements. Real-time GNSS techniques that rely on carrier phase measurements are highly vulnerable to signal propagation delays, both in Earth's atmosphere and in the local environment of the antennas. The pseudorange to a satellite j from a receiver station A using code and carrier-phase measurements is given by equations 1.1 and 1.2, respectively.

$$P_k^i = \rho_k^i + T_k^i + I_k^i + c\delta_k - c\delta^i + \nu_k^i. \tag{1.1}$$

$$L_{1k}^i = \rho_k^i + T_k^i - I_k^i + c\delta_k - c\delta^i + \lambda N_k^i + \nu_k^i, \tag{1.2}$$

where P is the pseudorange from code and L is the range measurement derived from carrier phase respectively. ρ_k^i is the true range to the satellite i from the receiver antenna k, T_k^i is the tropospheric error, I_k^i the ionospheric error, c the speed of light, δ_k the receiver clock correction, δ^i the satellite clock correction, λ the wavelength of the L_1 or L_2 carrier signal, N the respective carrier phase ambiguity and ν_k^i denotes the local effects influenced by the environment around the antenna such as multipath, diffraction and other biases such as receiver noise. Errors in these GNSS measurements are broadly classified as: satellite-based errors, propagation medium or atmospheric errors and receiver-based errors. Some of these errors can be nearly eliminated while others can only be reduced. Understanding of the significance of these errors is important for applications especially requiring high accuracy measurements. *The discussions in this chapter focus on GPS information primarily.*

Satellite based errors

There are five major types of satellite-based errors. They are: clock errors due to instability of onboard atomic clocks, ephemeris errors due to errors in the estimated satellite positions, instrumental bias due to RF components of satellite and receiver, relativistic effects due to different gravitational potential experienced by satellite and receiver clocks and selective availability (if any) due to intentional degradation of the GPS signal in frequency and time domain. Satellite geometry is also crucial for accurate measurements. The general overall GPS design was for unaided code observations and was specified to a global coverage with at least four satellites in view above five degrees elevation at 99.9% of the time [1].

Ephemeris error

While the ephemeris data is transmitted every 30 seconds, the information itself may be up to two hours old. Variability in solar radiation pressure has an indirect effect on GPS accuracy due to its effect on ephemeris errors. The satellite ephemeris is required for both pseudo range and phase computations. The master control station is responsible for estimating and updating the satellites ephemeris via broadcasted navigation data which can be used by real-time applications.

Clock error

The satellite clock error is the difference between the true GPS time and the time maintained by a satellite. Though the satellite contains highly stable atomic clocks, they drift with time. This drift is closely monitored by the monitor stations. The master control station estimates the drift and transmits clock correction parameters to the satellite for rebroadcast in the navigation message, which is used to correct the time and measurements in a receiver [2].

Atmospheric errors

The satellite signals propagate through atmospheric layers as they travel from the satellite to the receiver. Two layers are generally considered when dealing with GPS: the ionosphere, which extends from a height of about 50 to 1000 km above the Earth, and the troposphere which stretches to about 16 km above the equator and 9 km above the poles from the surface of the earth.

Ionospheric error

The ionosphere is a region of ionized gases (free electrons and ions). The principal source of ionization in the ionosphere is the electromagnetic radiation from the sun. As the GPS signal travels from the satellite to the receiver, the presence of free electrons in the ionosphere changes the velocity (speed and direction) of propagation of the signals. The change in signal speed changes the travel time of the signal, and therefore the apparent range to the satellite. The ionosphere is not uniform in composition, and the refractive index changes all along the path of a signal. The effect of signal bending causes a range error, which is quite substantial at very low elevation angles less than 5°. The ionosphere speeds up the propagation of the carrier phase beyond the speed of light, while it slows down the Pseudo Random Noise (PRN) code (and the navigation message) by the same amount. Therefore, the receiver-satellite distance will be too short if measured by the carrier phase and too long if measured by the code, as compared with the actual distance [3]. The ionospheric delay is proportional to the number of free electrons along the propagation path, which is known as the Total Electron Content (TEC). Further, this delay is dependent on three main factors: the geomagnetic latitude of the receiver, the time of day and the elevation of the satellite. A technique to remove a large part of the contribution from the ionosphere is to form a linear combination, L3, of the L1 and L_2 observables [4]

$$L_3 = 2.55L_1 - 1.55L_2. \tag{1.3}$$

It should be noted that due to such an approximation errors are introduced due to uncertainties involved in this computation.

Tropospheric error

The troposphere is the lower part of the atmosphere that is non-dispersive for frequencies up to 15 GHz. The troposphere causes a delay in both the code and carrier observations. Since it is not frequency dependent (within the GPS L band range) it cannot be canceled out by using dual frequency measurements, but it can, however, be successfully modeled accurately. The troposphere can be split into two parts: the dry component, which constitutes about 90% of the total refraction, and the wet part, which constitutes the remaining 10%. Values for temperature, pressure and relative humidity are required to model the vertical delay due to the wet and dry part, along with the satellite elevation angle, which is used with an obliquity/mapping function. The tropospheric error is computed by calculating a product of the zenith total delay (ZTD) with $m(\epsilon)$ (the mapping function).

Receiver based and local sources of error

Receiver based errors could be receiver noise caused due to limitations of receiver electronics, receiver clock error due to use of inexpensive crystal clocks, which are less accurate than that of the satellite clocks and improperly modeled antenna phase center variations. Antenna phase center for a receiver varies with frequency, elevation and azimuth and is difficult to model. Moreover, other unmodeled local sources of error, such as those due to the antenna environment, such as multipath and diffraction pose a hindrance to optimum position estimation using GNSS [5]. Multipath error occurs due to multiple signals reaching the GPS antenna upon reflection from ground, nearby buildings and structures. Reflected signals reaching the antenna have a path difference and phase difference with respect to the direct signal. The superposition of the reflected and direct signal gives a composite signal which is different in phase and amplitudes with respect to the direct signals. After arriving at the receiver antenna, the multipath signals propagate into the receiver where they distort the correlation function of the tracking loop. Subsequently, they cause biases in range and carrier-phase estimations. These range errors are intolerant for high-precision applications, such as earthquake monitoring, crustal deformation monitoring, etc., which require millimeter-level precision. Multipath effect is environment dependent and not spatially correlated and hence cannot be removed by using differential techniques. Various pre-receiver, in-receiver and post-receiver approaches are followed to mitigate the code and carrier Multipath error. The code Multipath errors for each satellite for successive days can be isolated by calculating the Code-Minus-Carrier values [4][6]. Multipath error repeats itself with each passing sidereal day if the environment around the antenna remains the same for successive days. Effective signal processing using adaptive filters for two successive days can extract out multipath. The calculated Multipath error is smoothened with Carrier smoothing filter to remove the high frequency receiver noise. Diffraction occurs when radio waves bend around an object. This could be caused by either natural or man-made obstructions to the Line-of-sight path to the GNSS signal, such as hills or buildings. The work done in Papers A and B explain a knife-edge diffraction model for signal diffraction and the discuss the degradation in GNSS positioning due to signal bending.

1.2 Differential GPS (DGPS)

Most of the error sources in GNSS can be eliminated or reduced using Real time Kinematic (RTK) network where GNSS carrier phase signals received at a stationary reference with known position coordinates are used to correct position data at a rover receiver in another location. Differencing measurements of two receivers to the same satellite eliminates satellite-specific biases; differencing between two satellites and one receiver eliminates receiver-specific biases. As a consequence, double-difference pseudoranges (as in RTK) are, to a high degree, free of systematic errors originating from the satellites and from the receivers [7]:

$$\nabla\Delta L^{ij}_{AB} = \nabla\Delta\rho^{ij}_{AB} + \nabla\Delta T^{ij}_{AB} - \nabla\Delta I^{ij}_{AB} + \nabla\Delta\lambda N^{ij}_{AB} + \nabla\Delta\nu^{ij}_{AB}. \tag{1.4}$$

Double differencing technique is used for cancelling out clock biases and minimizing atmospheric errors for short baseline lengths as shown in Equation 1.4 in which two satellites i, j and two stations A, B are used to compute the double differencing. The true length is given as a sum of true baseline length, the atmospheric errors and the error due to integer cycle ambiguity. Integer phase ambiguity is computed by using the code phase as a reference to the carrier phase. Since the atmosphere does not vary much for short baseline lengths, their error contribution to Equation 1.4 is minimal.

1.3 Real Time Kinematic (RTK)

Real Time Kinematic (RTK) is a system that utilises Global Navigation Satellite Systems (GNSS) carrier phase measurements to provide accurate positioning in real time.

The general idea in RTK is to receive GNSS carrier phase signals at a stationary reference with known position coordinates and to use these to correct position data at a roving receiver in another location. The ideal signal is perturbed by ionosphere, troposphere and imperfections related to ephemerides, clocks and multipath and thus the calculated position coordinates differ from the known coordinates. By calculating corrections that mathematically “move” the reference to its known position and subsequently apply a similar set of corrections to the rover, the rover’s position can also be determined very accurately. As the reference and rover are at different locations, the signals have been perturbed differently and the correction data are therefore affected by uncertainties that compromise the reliability of the rover’s corrected position. The factors that affect the uncertainties can be classified in different ways, e.g. distance dependent, systematic, random, site specific, rapid, frequency dependent (dispersive).

With RTK it is also implicit that, in addition to the broadcast code signals that are handled by relatively cheap off-the-shelf products, the carrier phase of the signal is analysed with a geodetic receiver. With this technique it is possible to obtain position coordinates with accuracy of order 1 cm. The difference between RTK and Network RTK (NRTK) is that the latter combines data from several reference stations to provide the rover with corrections. With NRTK the distance dependent errors are interpolated between the reference stations, which allows for increased distance between reference stations without losing position accuracy.

One such NRTK method builds on the concept of Virtual Reference Station, VRS. At the VRS, the rover calculates a position from uncorrected code data like any off-the-shelf receiver and uploads this navigated solution to the central unit. The central software then deploys a virtual reference station at the coordinates of the initial navigated solution on the common phase ambiguity level that is calculated from data from an appropriate combination of the surrounding reference stations. From the synthetic data of the calculated surface, the VRS emulates a real reference receiver at the initial navigated coordinates. The rover receives the VRS data and makes a phase adjustment of its own position on the relatively short baseline.

The knowledge of error sources and parameters discussed in Section 1.1 are essential since GNSS-based techniques are very vulnerable to errors arising from signal propagation delay in Earth atmosphere and in the local environment of the antennas. This is true both at the reference station and the rover. While the discussion on error sources in Section 1.1 are relevant for both code and carrier phase measurements, the primary focus of this work is using carrier phase measurements. This is because carrier phase measurements are often preferred over code measurements in precise positioning applications due to their improved signal resolution.

Among the various local environmental errors, diffraction remains particularly understudied, which motivates the objectives outlined below.

1.4 Research objectives

Given the gaps identified in the existing literature for the study of diffraction (see paper-A) as a distinct GNSS error source, this thesis pursues four primary objectives.

First, to demonstrate that signal diffraction is not merely a theoretical possibility but a measurable and significant error source in real-world GNSS positioning. While multipath has been extensively studied, diffraction has often been overlooked or incorrectly attributed. This work seeks to isolate diffraction effects using both real-world data and controlled experiments.

Second, to quantify how diffraction errors vary with the distance of an obstacle from the antenna. Specifically, this thesis investigates the relationship between obstruction proximity and the magnitude of positioning degradation, thereby providing practical guidance for field operations and antenna placement.

Third, to develop and validate physics-based models that capture the deterministic behavior of signals interfering in the near field of a GNSS antenna due to cylindrical obstructions. Unlike purely empirical corrections, these models aim to explain the underlying interference mechanisms, enabling better prediction and potential mitigation.

Fourth, to assess the practical implications of diffraction for key geodetic parameters, including coordinate positions and tropospheric delays. By understanding how diffraction biases these estimates, this research provides recommendations for processing strategies and elevation cutoff angles in obstructed environments.

Collectively, these objectives move beyond the traditional focus on multipath and establish diffraction as a distinct, model-able, and operationally relevant error source in high-precision GNSS geodesy.

1.5 Thesis outline

This thesis investigates signal diffraction as a distinct, quantifiable, and often unmodeled error source in high-precision GNSS geodesy.

This introductory chapter talks about the various types of GNSS error sources (satellite-based, atmospheric, and receiver/local errors), reviews differential GPS and RTK positioning, and concludes by framing the central challenge, study of diffraction as a primary error source.

Chapter 2 provides the theoretical foundation, first treating multipath due to reflections (signal model, power-delay profile, code vs. carrier phase errors, and mitigation strategies), then developing the physics of diffraction specifically knife-edge diffraction, and finally drawing a critical distinction between diffraction and multipath in the GNSS context before discussing implications for precise positioning and geodesy.

Chapter 3 describes the data processing methodology using two standard post-processing software packages: PPP with GipsyX, and network solutions with Bernese GNSS software, including pre-processing, ambiguity resolution, parameter estimation, quality control, and final network combination.

Chapter 4 summarizes the appended papers: Paper A investigates diffraction in complex real-world environments using double-difference residuals, PPP position estimates, and SNR data; Paper B presents a controlled experimental study with a movable wall, quantifying diffraction's inverse distance dependence and validating KED model limits; Paper C develops advanced phasor-based interference models for near-field diffraction from a cylindrical pole, achieving high-correlation empirical mapping. Paper D provides the foundational observational basis for edge diffraction, demonstrating signal degradation over metallic edges using multi-constellation GNSS data from construction equipment. Paper E extends the controlled experiments of Paper B to assess diffraction-induced biases in tropospheric zenith delay estimates, showing that nearby obstructions can inflate ZTD errors by up to 8 times and offering practical processing recommendations.

Chapter 5 offers concluding remarks and future work, followed by the full papers in Part II.

CHAPTER 2

Multipath and Diffraction

The mechanisms behind radio wave propagation are diverse, but this chapter aims to provide a preview of basic ideas behind reflection and diffraction in the context of this research.

2.1 Multipath due to reflections

Thanks to ongoing improvements from GNSS augmentations and modernization, many error sources have been reduced, leaving multipath as one of the most significant remaining error source for GNSS [8].

Multipath arises when a receiver captures reflected or diffracted signal replicas in addition to the direct line-of-sight signal. Thus, the GNSS antenna receives multiple, time-delayed replicas of the original signal alongside the direct-path signal. Once the lag of these replicas grows appreciable, such as past two times the code-chip interval for BPSK-R signals, the receiving equipment generally recognizes and removes them from consideration. Since the LOS signal always arrives first, such resolvable multipaths have little impact on performance as long as the receiver locks onto it.

Nonetheless, reflections from nearby objects, or even shallow-angle bounces off farther surfaces, can arrive at the antenna with only negligible lags of just tens or hundreds of nanoseconds after the direct signal. These closely spaced multiple paths alter the shape of the correlation function between the aggregate incoming signal (direct path plus multipath) and the receiver's locally generated reference. They likewise affect the phase of the aggregate signal, producing measurement discrepancies in pseudorange and carrier phase measurements that vary from satellite to satellite. Such disturbances therefore introduce inaccuracies in position, velocity, and time.

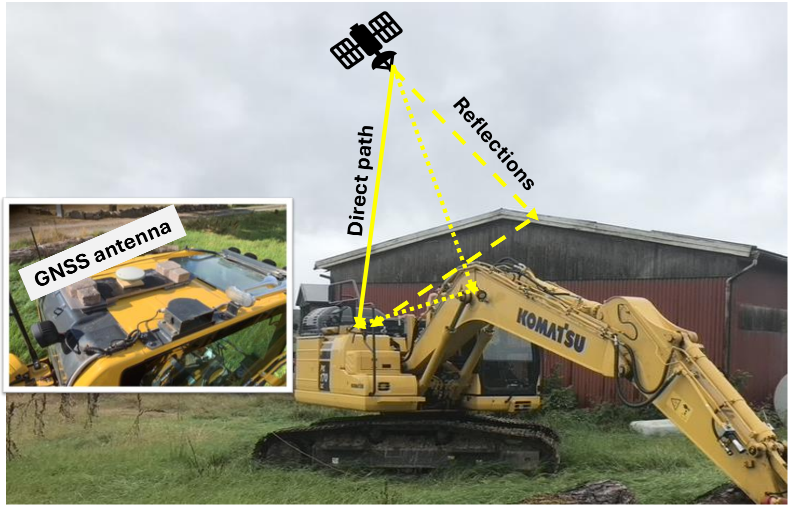

Figure 2.1: Multipath signal reception by the GNSS antenna mounted on an excavator (see inlay-ed image for top view of the antenna mount). While signal arrives via a direct path from the satellite, there are reflections from the neighboring environment including the metallic body of the excavator itself.

Standard evaluations of these reflection-induced impairments presume the direct ray experiences no loss, so that the reflected components carry less strength than direct path power.

The multipath signal model

The complex envelope of the received signal, $r(t)$, relative to a direct-path-only signal, is given by [8] as,

$$r(t) = \alpha_0 e^{-j\phi_0} \left[x(t-\tau_0) + \sum_{n=1}^{N} \tilde{\alpha}_n e^{-j\tilde{\phi}_n} x(t-\tau_0-\tilde{\tau}_n) \right] \tag{2.1}$$

Where,

- the direct path signal is given as, $\alpha_0 e^{-j\phi_0} x(t-\tau_0)$ and is the true signal that traveled along the LOS path. $x(t)$ is the complex envelope of the transmitted signal, α_0 is its amplitude, τ_0 is its propagation delay (the true measurement of interest), and ϕ_0 is its carrier phase.

- The number of multiple paths (N) form the upper bound of the summation, representing the total number of reflected (or diffracted) signal copies being received.

- The Multipath-to-Direct Ratio (MDR, $\tilde{\alpha}_n$) is defined as $\tilde{\alpha}_n = \alpha_n/\alpha_0$ and is the dimensionless amplitude of the n-th multipath signal relative to the direct signal's amplitude. If $\tilde{\alpha}_n$ is close to 1, the multipath is nearly as strong as the direct signal, posing a significant threat.

- Excess Delay ($\tilde{\tau}_n$) is defined as $\tilde{\tau}_n = \tau_n - \tau_0$ and is the additional propagation delay of the n-th multipath relative to the direct path. Since a reflected path is always longer, $\tilde{\tau}_n > 0$. Short-delay multipaths (e.g., a few nanoseconds to tens of nanoseconds) are the most difficult for a receiver to separate from the direct signal.

- Relative Phase ($\tilde{\phi}_n$): The carrier phase of the n-th multipath signal relative to the direct signal. This parameter is critically important, as it dictates whether the multipath signal combines with the direct signal constructively (causing a signal power increase) or destructively (causing deep signal fading and maximum ranging error).

The multipath Power Delay Profile (PDP)

The Power-Delay Profile (PDP) offers a practical way to characterize a static multipath environment by visualizing how the channel responds to an impulse. Specifically, it plots the received power of each multipath component (represented by the squared amplitude $\tilde{\alpha}_n^2$) against its corresponding excess delay $\tilde{\tau}_n$. $\tilde{\tau}_n$, as explained before, measures how much later the n^{th} echo arrives compared to the direct line-of-sight signal. The resulting graph directly reveals the structure of the multipath channel, showing how many reflections are present, how strong they are, and how they are distributed in time. From this profile, two useful summary metrics can be derived. The first is the multipath spread, which is simply the total range of excess delays over which the PDP is essentially non-zero. This indicates the overall time span of the channel's echoes and gives a sense of how long the signal energy lingers. The second metric is the RMS delay spread, a more refined statistical measure that captures the time dispersion of the channel. It is calculated as the root-mean-squared spread of the excess delays, weighted by their corresponding powers, and is defined mathematically as,

$$\tau_{\text{rms}} = \sqrt{\frac{\sum_n \tilde{\alpha}_n^2 \tilde{\tau}_n^2}{\sum_n \tilde{\alpha}_n^2} - \left(\frac{\sum_n \tilde{\alpha}_n^2 \tilde{\tau}_n}{\sum_n \tilde{\alpha}_n^2}\right)^2} \tag{2.2}$$

Unlike the simple multipath spread, the RMS delay spread condenses the entire delay-power distribution into a single number, offering a compact and meaningful indicator of how severely the channel will distort GNSS signals. Together, these metrics help a receiver designer or a field engineer assess the multipath environment and anticipate its impact on code and carrier tracking performance.

Code vs carrier phase multipath error

Multipath affects a receiver's code and carrier measurements in two different ways. For the code measurement, the receiver determines the signal's arrival time by generating an internal reference code and aligning it with the incoming satellite signal, thus computing a correlation peak. The direct signal creates a clean, sharp peak. The reflected signal creates a delayed, distorted copy of that peak. When these two peaks overlap, they blend together erroneously into a single, distorted peak. The receiver's tracking loop is designed to lock onto what it thinks is the top of the peak. Because the shape is distorted, the receiver prompt fixes on the wrong spot. The code multipath error is the time difference between where it locked on and where the true peak from the direct signal should have been. Its magnitude is relatively large, on the order of meters, and is highly dependent on the signal's modulation and bandwidth.

Multipath affects not only pseudorange but also carrier phase measurements. The receiver's phase-locked loop (PLL) tracks this composite signal which is formed by the sum of phasors of the direct and reflected signals, deviating the measured phase away from the true value. For a single multipath reflection, the resulting carrier phase error ψ is given by [8] as,

$$\psi = \tan^{-1}\left[\frac{\tilde{\alpha}_1 \sin(\tilde{\phi}_1) R_x(\epsilon - \tilde{\tau}_1)}{R_x(\epsilon) + \tilde{\alpha}_1 \cos(\tilde{\phi}_1) R_x(\epsilon - \tilde{\tau}_1)}\right] \tag{2.3}$$

where $\tilde{\alpha}_1$ is the MDR, $\tilde{\phi}_1$ the relative phase, $\tilde{\tau}_1$ the excess delay, ϵ the code tracking error, and $R_x(\cdot)$ is the normalized autocorrelation function of the spreading code. It describes how well the incoming signal correlates with the locally generated replica at a given offset.

A key property of carrier phase multipath error is that it is bounded within limits. Unless the reflected signal is stronger than the direct signal ($\tilde{\alpha}_1 \leq 1$), using Eq 2.3, one can see that the carrier phase error can never exceed

90°. So, its magnitude is fundamentally limited to a quarter of a carrier wavelength (approximately 5 cm for GPS L1). Thus it is much smaller than code multipath error but still, it is the dominant error source in high-precision applications like Real-Time Kinematic (RTK) positioning.

However, there is always the possibility of a worst case scenario when the multipath signal has equal strength as the direct signal ($\tilde{\alpha}_1 = 1$)and is 180° out of phase. With low-elevation satellites, a strong, short-delay reflection can combine destructively with the direct signal, causing severe fading and potential loss of lock [8].

Multipath mitigation

One effective strategy for managing multipath is to prevent reflected signals from entering the receiver antenna altogether, thereby reducing the need for complex internal processing. Practical measures include selecting an optimal antenna location or altering nearby reflective surfaces—for instance, by applying radio-frequency absorbing coatings—which can greatly reduce multipath effects. Also, choke ring antennas are particularly successful at attenuating multipath signals originating from the ground or from low-elevation scatterers. Since reflections invert the polarization of electromagnetic waves, these antennas can be engineered to block left-hand circularly polarized signals, further minimizing interference.

In short-baseline differential setups, multipath errors at a stationary reference station can be mitigated through calibration. By characterizing the multipath error as a function of satellite position, one can apply appropriate corrections [9].

Receiver-based multipath mitigation strategies divide into two main classes: nonparametric and parametric processing. Parametric processing works by first estimating the parameters of each multipath component and then compensating for their influence on the direct signal's time-of-arrival estimate. Most parametric methods rely on a discrete multipath model, such as the one presented in Eq. 2.1. These algorithms either assume a fixed number of multipath signals or estimate that number, along with parameters like the multipath-to-direct ratio, excess delay, and relative carrier phase for each reflected path. Nonparametric processing, by contrast, uses discriminator designs that are naturally less vulnerable to multipath-induced distortions. These methods require accurate prior knowledge of the signal's ideal correlation function and then attempt to fit that function to the observed correlation under multipath conditions. The most common nonparametric techniques are variants of early-late processing. They enhance the narrow correlator approach either by applying time-gating to the reference signal or by calculating two pairs of early and late correlations with distinct spacing. As an example the Multipath Estimating Delay Lock Loop (MEDLL) [10] employs maximum likelihood estimation to minimize the mean-squared error between the received signal (modeled as in Eq. 2.1) and a locally generated reference replica. Other methods have also been introduced [11] and have been demonstrated to minimize both mean-squared error and root-mean-squared error.

2.2 Diffraction

Radio waves can be received in shadowed regions even if there is no line of sight between the transmitting source and the receiving antenna. This is different from multipath since there is no direct LOS path and is extremely dangerous for the receiver since the delayed path is then mistaken as the LOS path by the receiver. In the absence of LOS, reflections from the surface of other objects could also contribute signal reception in shadowed regions. However, diffraction is a very significant mechanism which enables radio signals to travel around obstructions and thus arrive at the receiver even in regions where signal availability is unexpected.

Diffraction can be well understood using Huygen's principle. According to this principle, all points on a wavefront act as point sources for the production of secondary wavelets. These wavelets combine to produce a new wave along the direction of propagation. Diffraction is caused by the propagation of secondary wavelets into a shadowed region [12]. To study this propagation, this research work adopts a simplified scenario known as knife-edge diffraction, which can be conservatively applied to estimate realistic effects. In the Knife-edge model, the obstruction is assumed to be sharp and is located along the line-of-sight path between the receiver and the transmitter (satellite). Additionally, for this model, it is assumed that the obstruction has infinite width and that no signals penetrate through it to reach the receiver.

Knife edge diffraction

The side view of a typical knife edge obstruction is shown in Fig. 2.2. The transmitter T and the receiver R are at different heights with respect to the horizontal plane as can be expected. P is the point for the top of the diffracting knife edge. From the knife edge, the distance to the transmitter is assumed to be r_1 and that to the receiver antenna is r_2. While TR is the LOS path, which is blocked by the obstruction, the bent path due to diffraction is via TPR.

The diffraction geometry of triangle TPR maybe simplified as shown in Fig. 2.3. It should be noted at this point that in the context of GNSS, the

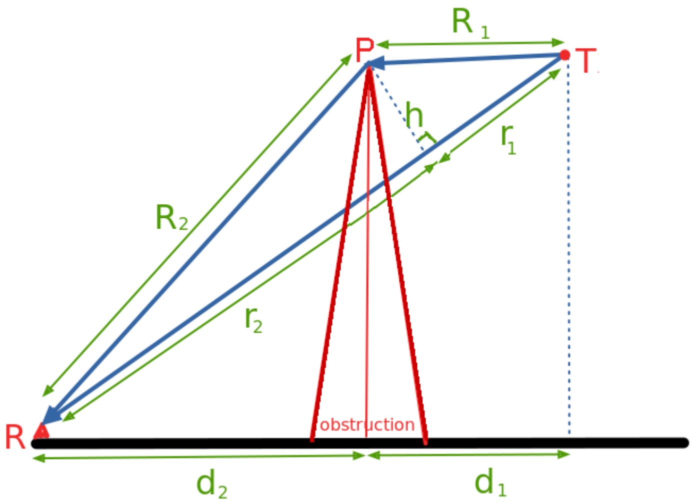

Figure 2.2: Knife edge diffraction model

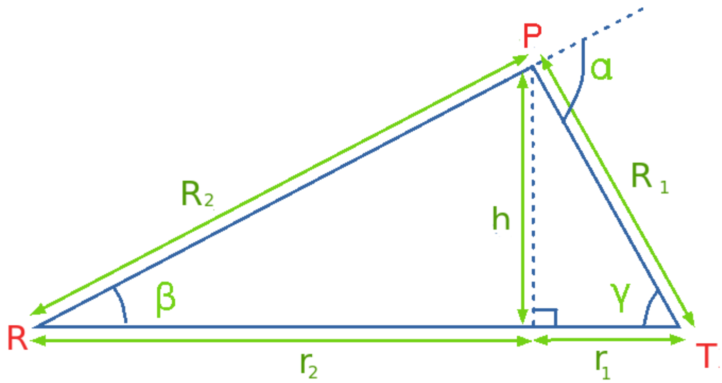

Figure 2.3: Simplified Knife edge geometry.

transmitter is located at a much larger distance r_1 than the receiver distance r_2. For the specific case of GNSS, Fig. 2.2 can be modified as shown in Paper-A, Fig. 1(a). Also, both r_1 and r_2 are much larger than h. Here, we derive general equations for the path delay and the Fresnel-Kirchhoff diffraction parameter using a knife edge model. These equations are modified for a GNSS context and used in Paper-A.

The extra path length, Δ traveled by the signal due to diffraction maybe computed as shown in [12].

$$\begin{aligned}
\Delta &= (R_1 + R_2) - (r_1 + r_2) \\
&= \sqrt{r_1^2 + h^2} + \sqrt{r_2^2 + h^2} - (r_1 + r_2) \\
&= r_1\sqrt{1 + \frac{h^2}{r_1^2}} + r_2\sqrt{1 + \frac{h^2}{r_2^2}} - r_1 - r_2 \\
&\approx r_1\left(1 + \frac{h^2}{2r_1^2}\right) + r_2\left(1 + \frac{h^2}{2r_2^2}\right) - r_1 - r_2 \\
&= \frac{h^2}{2}\left(\frac{1}{r_1} + \frac{1}{r_2}\right) \\
&= \frac{h^2}{2}\frac{r_1 + r_2}{r_1 r_2}
\end{aligned} \tag{2.4}$$

The angle $\alpha = \beta + \gamma$. Since $r_1, r_2 \gg h$,

$$\begin{aligned}
\beta &= \tan^{-1}\frac{h}{r_2} \approx \frac{h}{r_2} \\
\gamma &= \tan^{-1}\frac{h}{r_1} \approx \frac{h}{r_1} \\
\alpha &\approx \frac{h(r_1 + r_2)}{r_1 r_2}
\end{aligned} \tag{2.5}$$

The corresponding phase difference is equal to

$$\phi = \frac{2\pi}{\lambda}\Delta = \frac{2\pi}{\lambda}\frac{h^2}{2}\frac{r_1 + r_2}{r_1 r_2} = \frac{\pi}{2}h^2\frac{2}{\lambda}\frac{r_1 + r_2}{r_1 r_2} \tag{2.6}$$

Eq. 2.6 can be normalized by defining the dimensionless Fresnel - Kirchhoff diffraction parameter as,

$$\nu = h\sqrt{\frac{2(r_1 + r_2)}{\lambda r_1 r_2}} = \alpha\sqrt{\frac{2r_1 r_2}{\lambda(r_1 + r_2)}} \tag{2.7}$$

This equation is later made use of in Paper A and B, for modeling diffraction. The phase difference ϕ can be expressed in terms of ν as,

$$\phi = \frac{\pi}{2}\nu^2 \tag{2.8}$$

Thus, both the height and placement of an obstruction, along with the transmitter and receiver geometry, determine the phase shift between the direct and diffracted propagation paths. This is studied in further detail in Papers A and B in a complicated and a controlled environment respectively.

2.3 Diffraction vs multipath in the context of GNSS

Both diffraction and multipath degrade GNSS positioning, but they are fundamentally different phenomena. Multipath is the superposition of direct and reflected signals. Diffraction, in contrast, occurs when the direct path is completely blocked and the signal reaches the antenna only by bending around an obstacle [13]. This distinction leads to different ranging error characteristics.

For multipath, the pseudorange error can be positive or negative and is bounded by half a code chip [14]. The carrier phase error is fundamentally limited to a quarter of a wavelength, or approximately 5 cm for GPS L1 [8]. Non-line-of-sight (NLOS) reception caused by diffraction behaves differently: the pseudorange error is always positive and equals the additional path delay, typically ranging from several meters to tens of meters [15]. While NLOS carrier phase error is presumed to behave similarly, limited research exists on the topic [16].

Diffraction poses a particularly difficult challenge for high-precision positioning. It can introduce path delays at the decimeter to centimeter level [17] and cause rapid phase fluctuations, significant amplitude attenuation, and cycle slips [18]. Signal strength can be reduced by up to 17 dB-Hz [19]. Studies suggest that diffraction impacts can exceed those of multipath, reaching magnitudes of several carrier wavelengths with complex fluctuation patterns [20]. [21] proposed a geometrical model to extract and characterize diffraction errors, showing they often follow a monotonic trend and can reach 50–200 mm. However, their approach does not incorporate the underlying physics of wave propagation or use supportive metrics such as the signal-to-noise ratio (SNR). Certain model predictions—such as error increasing with horizontal distance to the obstruction or being larger for high-elevation satellites—appear to contradict both diffraction theory and practical experience, where nearby obstacles and low-elevation signals pose greater threats. These discrepancies highlight the need for diffraction models that involve an understanding of wave propagation physics.

2.4 Impact on precise positioning and implications for geodesy

In high-precision real-time GNSS applications, an elevation cutoff angle of 10° to 15° is typically used to reject low-quality signals. Users such as machine guidance systems rely on GNSS data every second. However, surrounding objects, including the machine itself, often cause multipath and diffraction effects that can introduce coordinate errors of several centimeters or even decimeters.

While multipath is a well-known challenge for construction equipment like excavators and cranes, diffraction is either overlooked or poorly understood. A notable gap remains in isolating diffraction from other local environment signal degradation phenomena. Most modern studies treat diffraction as part of a broader urban signal degradation model, and diffraction-specific research remains underdeveloped. This motivates the studies carried out in Papers A, B, and C. Although typically short-lived, diffraction can significantly impact the accuracy of RTK and Network RTK (NRTK) measurements.

Diffraction introduces a slowly varying, systematic bias into the measurements. Unlike random noise, this error is deterministic and structured, meaning it cannot be averaged out and requires physical or empirical modeling. It also compromises the integer nature of carrier-phase ambiguities, leading to fix failures or biased fixed solutions. Furthermore, excellent satellite geometry with low Dilution of Precision (DOP) can coexist with large systematic errors, demonstrating that low DOP is a necessary but not sufficient condition for high accuracy [22].

Beyond positioning, unmodeled diffraction may be absorbed into estimated tropospheric parameters. For geodetic-grade applications, the antenna environment must be free not only of obstructions but also of near-grazing diffracting edges. A single affected station can introduce biases that propagate into a larger geodetic network solution, degrading products for all users. Over decades, this small bias can accumulate into a significant positional error, compromising the reference frame and studies such as crustal deformation, sea-level rise, and post-glacial rebound.

CHAPTER 3

Data processing using GNSS post processing software

Post-processing of GNSS carrier phase data helps in precise estimation of position. Scientific software commonly used for GNSS post-processing such as GipsyX software [23] and Bernese GNSS software [24] have been used in papers A, B and C and are discussed here. This chapter also provides information on external sources of data required to achieve high precision.

3.1 External information required in high precision applications and their sources

High-precision post-processing applications of GNSS data require accurate information about the GNSS satellite orbits and clocks. Since the accuracy of the broadcast orbit information is at meter-level this study utilizes final orbit and clock products from the International GNSS service (IGS) [25] which has uncertainties on the order of 1-2 cm. The orbit and clock products are calculated at the IGS analysis center. The final products can only be used for post-processing, since they have a latency of approximately 14 days. The precise final products for the satellites' orbits and clocks are downloaded from the IGS, together with the other products needed to reach sub-centimeter precision.

The second source of external information comes from International Earth Rotation and Reference System Service (IERS) [26] which provides information about the solid earth tides, ocean tide loading and the Earth Orientation

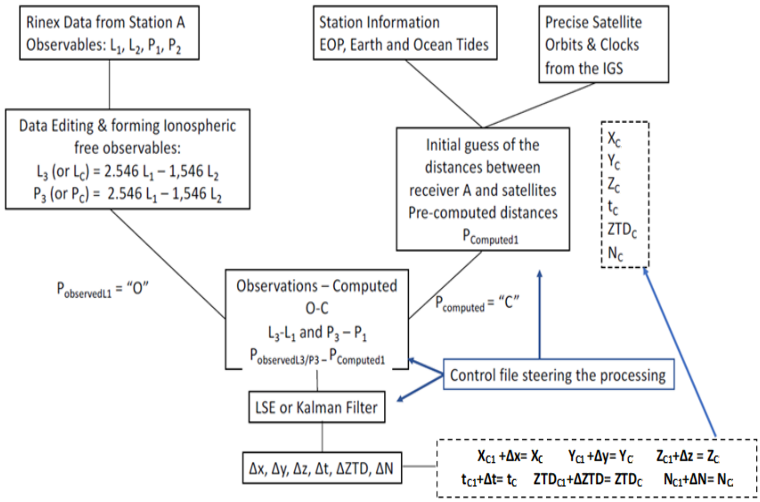

Figure 3.1: Flowchart for the GipsyX software

Parameters (EOP). In geodesy, EOP illustrate irregularities in earth's rotation. EOP provides the rotational transform from the International Terrestrial Reference System (ITRS) to the International Celestial Reference System (ICRS), or vice versa, as a function of time. Solid earth tides are the displacement of the earth's surface due to the influence of the Sun's and the Moon's gravitational forces. Displacements are also caused by ocean tidal loading. Internationally agreed models for reference frames, EOP, solid earth tides, and ocean tide loading are implemented in all high-precision geodetic software packages. These models are constantly revised and update by the IERS, in the so called IERS conventions [27]. Software packages like the Bernese Software and GipsyX have the same and latest IERS models implemented.

3.2 Precise point positioning (PPP) using GipsyX software

The workflow using GipsyX software has been illustrated in Figure 3.1. Raw data files logged in GNSS receiver in RINEX (Receiver Independent Exchange) format, are fed to GipsyX. Most geodetic processing software for GNSS data use a well-defined set of observables as shown in Figure 3.1:

- the carrier-phase measurement at one or both carriers seen as L_1 and L_2
- the pseudorange (code) measurements P_1 and P_2 (for L_1 and L_2 respec-

tively)
- the observation time

The observation time is valid for both the phase and the code measurements, and for all satellites observed. Apart from the observations on code and carrier phase, information such as station-related information like station name, antenna height, etc. are obtained from the RINEX file. Each individual station, designated as A in Figure 3.1 is processed one at a time to obtain the observables L_1, L_2, P_1, P_2. The data is then edited to from linear combinations for L_3 and P_3 which are ionosphere free observables using equations shown in Figure 3.1. As stated earlier in Equation 1.3, such editing involves error inclusion due to approximations. Coordinates from RINEX header are used as an initial guess for the station position. Since we process 24 hour data, during which the station moves due to earth's rotation, effects of different geophysical phenomena (such as earth and ocean tides, etc.) and earth orientation parameters will change during the day. GipsyX uses standard models to eliminate these effects. IGS product files such as precise orbits and clocks are also used as inputs for computation. Using all these inputs, pseudorange distances based on code and carrier phase measurements between receiver A and satellites are computed. Such a computation also involves computing initial guesses of all the parameters of interest namely the co-ordinates (X_{C1}, Y_{C1}, Z_{C1}), the time information (t_C1), the Zenith Tropospheric Delay (ZTD_{C1}) and the integer ambiguity for carrier phase data (N_{C1}). The pre-computed values(¨C¨) are then subtracted out of the observables (¨O¨). These differences are then processed in Least square estimator (LSE) or a Kalman filter. The filter uses a user defined input control file to understand the parameters of interest. Thus, the outputs of the filter are the changes in parameters of interest namely Δx, Δy, Δz, Δt, ΔZTD, ΔN. These changes are then used to update the initial guesses to form freshly computed values (so X_{C1} modifies to X_{C2} and so on) and with every iteration the computed values get closer to the true values. The process is repeated until the statistics around the computed solution X_C, Y_C, Z_C, t_C, ZTD_C, N_C is satisfactory enough. Papers A, B and C use GipsyX position estimates to study the impact of diffraction.

3.3 Network solution using Bernese GNSS software

Figure 3.2 shows the flow chart for processing using Bernese GNSS software (BSW). While the precise point positioning (PPP) algorithm is similar to that of GipsyX, BSW also provides the possibility to estimate a network

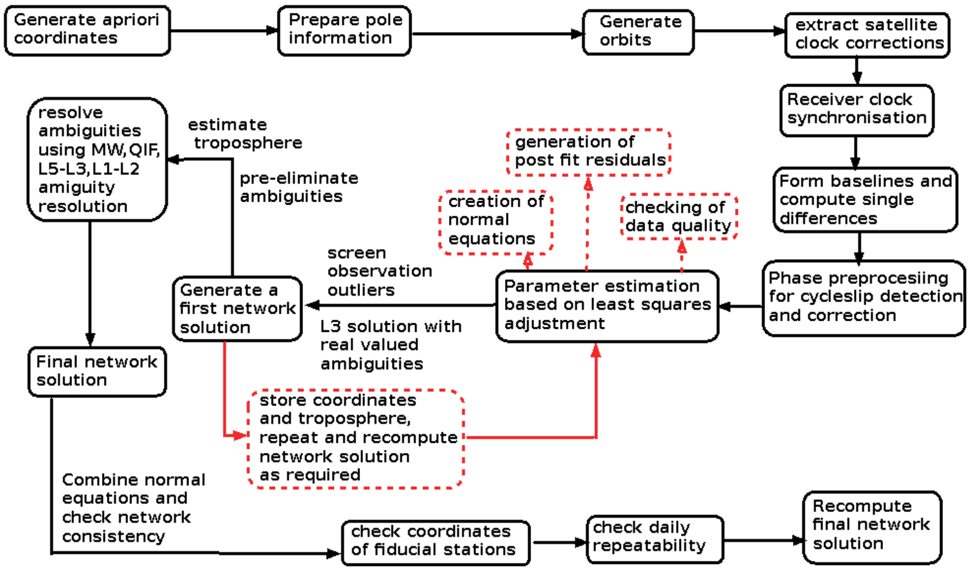

Figure 3.2: Flowchart for the Bernese GNSS software

solution using single frequency data which is advantageous for isolating local unmodeled effects such as multipath and diffraction using a double difference solution of colocated stations. This is made use of in Papers A, B and C to study diffraction effects in GNSS signals.

The Bernese GNSS Software processes network solutions through a sequence of well-defined steps, as outlined below.

Preprocessing

A priori coordinates for all stations are introduced, together with pole information and precise satellite orbits. Satellite clock corrections are extracted for consistency checks. Receiver clocks are synchronised to ensure proper alignment of observations.

Ambiguity resolution and parameter estimation

Phase ambiguities are resolved using multiple methods, including the Melbourne–Wübbena combination, the quasi-ionosphere-free approach etc. Troposphere parameters are estimated while ambiguities are pre-eliminated. Normal equations of the form $\mathbf{N} \cdot \mathbf{x} = \mathbf{b}$ are then created for each baseline or subnetwork, where $\mathbf{N}$ is the normal matrix containing the weighted correlations between parameters, **x** is the vector of unknown station coordinates, troposphere delays, and ambiguities, and **b** is the right-hand side vector derived from the observed minus computed observations.

Quality control

Post-fit residuals are generated and used to check data quality. Phase preprocessing detects and corrects cycle slips. Baselines are formed and single differences are computed in preparation for the final adjustment.

Final network combination

A final network solution is computed. Normal equations from different sessions are combined, and network consistency is verified. Daily repeatability is examined to identify any remaining issues. If necessary, the final network solution is recomputed to ensure a consistent and high-precision result.

This processing strategy delivers reliable station coordinates and troposphere estimates suitable for geodetic reference frame maintenance and deformation monitoring.

The majority of GNSS error sources can be rigorously modeled and mitigated by postprocessing software such as Bernese GNSS software or GipsyX software. However, signal degradation due to fading caused by the local environment around the antenna continues to pose a problem. Both reflections and diffraction from surrounding objects interfere with the line-of-sight GNSS signal, degrading the positioning accuracy even in a post-processing mode. This is studied in Papers A and B. In general, it is difficult to make very precise estimates of diffraction error. In practice, prediction involves a process of theoretical approximation, modified by necessary empirical corrections [28], similar to the approach used in Paper C for the study of diffraction caused by a pole. Paper E further shows that diffraction biases not only positions but also tropospheric estimates (obtained using PPP estimates made by PRIDE software), with ZTD errors increasing up to 8-fold in obstructed environments.

CHAPTER 4

Summary of included papers

This chapter provides a summary of the included papers.

4.1 Paper A

> **Uttama Dutta**, Jan Johansson, Rüdiger Haas
> Investigating the impact of diffraction on GNSS carrier phase measurements
> *Journal of Geodesy*, vol. 100, no. 4, SP 25, April 2026.
> This document is the 'Accepted Manuscript' version. The 'Version of Record' of this article is available online at:
> https://doi.org/10.1007/s00190-026-02045-w .

In this paper, we investigated whether signal diffraction, a phenomenon often overlooked in GNSS error budgets, significantly degrades high-precision positioning. We began with the fact that while standard post-processing corrects for large-scale errors such as satellite orbits, clocks, and atmospheric delays, localized diffraction effects remain largely unmodeled. Unlike random noise, diffraction introduces a slowly varying, systematic bias that cannot be averaged out. Using both long-term real-world datasets and synthetically modified data, we analyzed double-difference carrier phase residuals, PPP position estimates, and SNR measurements. Our analysis revealed that diffracted signals are indeed received in areas where the direct line of sight to the satellite is obstructed. When these bent signals are inadvertently included in positioning solutions, standard algorithms fail to correct for them, leading to significant errors that depend heavily on the antenna's local environment. Through simulations, we demonstrated that position estimate scatter can double in the presence of non-minimal diffraction effects. We confirmed this degradation using real data as well. A key methodological choice we made was to avoid position estimation using double differences, which preserved the diffraction-induced error signature within the carrier-phase residuals clearly. We further supported our findings by analyzing SNR measurements alongside precise Lidar-scanned environmental data, which confirmed that the observed residual anomalies were directly attributable to physical diffraction from the obstruction. Overall, this paper established that diffraction is not a negligible effect but a critical factor that can compromise the accuracy of precise GNSS applications. It also provided a reproducible processing framework and set the stage for the controlled experiments that followed in the subsequent papers.

I led the conceptualization of this study and developed the methodology. I carried out all investigations, including the analysis of real-world and synthetic datasets. I performed data curation, validation, and formal analysis, and I created all visualizations. I wrote the original draft and handled subsequent review and editing with my coauthors. The role of my coauthors is as follows: J.J. provided resources, supervised the research, and contributed to review and editing. R.H. contributed to the conceptualization of the simulation studies and assisted with review and editing.

4.2 Paper B

Uttama Dutta, Jan M. Johansson, Rüdiger Haas, Sten E.G. Bergstrand, Carsten Rieck
Experimental Characterization of GNSS Carrier Phase Diffraction Errors in a Controlled Environment
GPS Solutions. in review .

Building directly on the findings of Paper A, in this paper we designed and conducted a controlled experiment to isolate diffraction effects with greater precision than was possible using real-world urban data alone. While Paper A had demonstrated that diffraction degrades positioning accuracy in complex environments, the presence of multiple obstructions made it difficult to quantify the effect purely as a function of obstacle geometry and distance. To address this limitation, we constructed a movable metallic wall of constant height and placed it on the southern side of a geodetic antenna. We created five distinct diffraction scenarios by moving the wall from 1 m to 3 m distance, each compared against an unobstructed reference case. Using dual-frequency

PPP and single-frequency double-difference analysis, we systematically extracted diffraction-induced errors. Our results empirically confirmed a key prediction from Paper A: PPP position errors can double when a diffracting wall is positioned at 1 m distance. We also demonstrated that diffraction impact is inversely proportional to obstacle distance, with errors at 1 m far exceeding those at 3 m. Furthermore, we showed that signal disturbance begins when an obstacle intrudes upon the first Fresnel zone, even while remaining below the direct line of sight, and that low-elevation satellites suffer the most severe effects due to their longer propagation paths through the diffracted field. We applied the Knife-Edge Diffraction (KED) model to our SNR observations and found that while the model works well for horizontal distances of 2 m, it requires improvement for near-field obstructions at 1 m. Based on our extensive analysis, we proposed a practical guideline for field operations: the obstructive environment should not subtend an angle greater than 11° on the antenna to ensure data integrity in demanding applications such as PPP and RTK. We also validated our earlier proposition that Dilution of Precision (DOP) alone is an insufficient metric for assessing positioning reliability in obstructed environments.

For, this paper, I conceptualized the study and developed the methodology. I conducted the controlled wall experiment, performed the investigations, and handled the validation, and formal analysis. I was also responsible for gathering the data from the no-network remote location at the observatory in all weather conditions, pre-processing and storing it. I created all visualizations, wrote the original draft, and participated in review and editing with my coauthors. The role of my coauthors is as follows: J.M.J. provided resources, supervised the research, and contributed to review and editing. R.H. supervised the research and assisted with review and editing. S.E.G.B. contributed to review and editing. C.R. contributed to review and editing.

4.3 Paper C

Uttama Dutta, Jan M. Johansson
Study of GNSS Phase Center Perturbations from Cylindrical Obstructions
Journal of Geodesy. in review .

In this paper, we extended our experimental approach to a different obstruction geometry: a cylindrical pole of 2 m height placed at 1 m distance from the antenna. Our goal was not merely to quantify diffraction errors but to develop a physics-based model that could capture the deterministic behavior of diffracted signals. Using long-term data collected with and without the pole, we differenced the measurements to generate high-resolution maps of phase variation across azimuth–elevation space. These empirical maps revealed a complex interference pattern arising from two distinct mechanisms: top diffraction producing concentric rings around the pole direction, and vertical edge diffraction generating wedge-shaped fringes periodic in azimuth. We then developed a series of phasor-based interference models of increasing physical realism. Starting from simple single-edge diffraction, we progressively incorporated region-specific physics, finite-diameter edge asymmetry, cylindrical scattering phase shifts, narrow-band optimization, and elevation modulation. Each step incrementally improved the model's alignment with the true electromagnetic interaction. The correlation with our empirical data jumped from 0.202 to 0.613, with the final hybrid model achieving an RMS error of 1.74 mm over the full sky. Within the critical azimuth sector of 180–220°, where scattering was strongest, the correlation improved further to 0.689. A key contribution of this work was demonstrating that a simple parametric model, with diffraction amplitudes and phase shifts calibrated directly against observed phase variations, could capture the full diffraction signature with high accuracy, sidestepping the complexity of a full forward model. The optimized phase shifts provided insight into the interaction mechanisms, including evidence of asymmetric near-field coupling between the cylinder and the antenna. This paper showed that near-field scattering from a metallic object is not an unpredictable error source but a deterministic phenomenon that can be modeled and potentially corrected.

For this paper, I led the conceptualization and methodology, carried out the investigation, validation, formal analysis, and visualization. I was also responsible for gathering the data from the no-network remote location at the observatory in all weather conditions, pre-processing and storing it. I also wrote the original draft. Together with my coauthor I reviewed and edited the manuscript. My coauthor J.M.J. provided the necessary resources, supervised the research and contributed to review and editing.

4.4 Paper D

Uttama Dutta, Jan Johansson
Multi-Constellation/Multi-Frequency GNSS Signal Degradation Due to Foliage and Reflective Environments
Engineering Proceedings, vol. 54, no. 1, p. 2, Sep. 2023.
https://doi.org/10.3390/ENC2023-15454 .

This paper presents initial observational work conducted as part of the SiL 2.0 project. The study examines multi-constellation (GPS and Galileo) and multi-frequency signals received on a GNSS antenna mounted on stationary construction equipment. Using signal strength indicators (SSI), the paper characterizes signal behavior in the presence of foliage and reflective surfaces around an excavator. A consistent observation is that traditional GPS L2 signals (C2W and L2W) appear weaker than L2C and L1 C/A signals across the tracked GPS satellites. The paper also briefly discusses signal bending over sharp metallic edges. This simple edge-bending concept later informed the more detailed diffraction studies presented in the papers A and B of this thesis. This work helped motivate the controlled experiments and modeling efforts that followed in papers A, B, C.

The document is based on the foundational work carried out by me under the supervision of my coauthor.

4.5 Paper E

Uttama Dutta, Jan M. Johansson, Peng Feng
Impact of Diffraction on GNSS Troposphere Estimates in a Controlled Environment
Manuscript to be submitted .

Having established in Papers B and C that diffraction significantly affects carrier phase measurements and positioning coordinates, we turned our attention in this paper to a less explored question: how does diffraction bias tropospheric estimates obtained from PPP? We leveraged the same controlled experimental setup from Paper B, the movable metallic wall placed on the southern side of the antenna at distances of 1 - 3 m alongside a reference station measuring identical atmospheric conditions without any obstruction. This design allowed us to isolate diffraction-induced tropospheric errors from true atmospheric signals. Our initial results are interesting. At a wall distance of 1 m, differential zenith tropospheric delay errors increased 4 to 8 times compared to the baseline unobstructed case, with RMS errors reaching up to 2.6 mm. Counterintuitively, raising the elevation cutoff from 5° to 10° didnot reduce the diffraction impact, particularly when tropospheric gradients were estimated. When we moved the wall to 2 m, however, the differential ZTD errors reduced below 1 mm. Work is still ongoing and the paper is soon to be submitted. Based on the tentative findings, we recommended that practitioners operating in obstructed environments use a 5° elevation cutoff without gradient estimation to minimize diffraction-induced biases in tropospheric estimates. This work demonstrates that diffraction errors are not limited to positioning coordinates but propagate directly into derived geodetic products, with implications for any study relying on high-accuracy tropospheric delays from GNSS measurements in less-than-ideal environments.

The work on the manuscript is still ongoing. However, the conceptualization, and methodology of the attached draft was led by me. I also carried out the investigation, validation, formal analysis, and visualization. Moreover, I was responsible for gathering the data from the experiment site at the observatory, pre-processing and storing it. Finally, the original first draft was prepared by me. Together with my coauthors, I reviewed and edited the manuscript. J.M.J provided the resources, supervised the research and contributed to review and editing. P.F. wrote the section on 'PPP troposphere estimation with PRIDE' and a part of the introduction in the original draft and also contributed to review and editing.

CHAPTER 5

Concluding Remarks and Future Work

This thesis shows that GNSS signal diffraction is a distinct, deterministic, and often unmodeled error source that degrades high-precision geodetic positioning. Across four interconnected studies, ranging from real-world urban observations to controlled experiments with movable walls and cylindrical poles, we have shown that diffraction introduces slowly varying, systematic biases into carrier-phase measurements that persist even after double-differencing and cannot be averaged out over time. Near-field obstructions (at 1 m) produce complex interference patterns (concentric rings and wedge-shaped fringes) that our physics-based phasor models captured with correlations exceeding 0.61 and RMS errors below 2 mm. Furthermore, we quantified how diffraction aliases into tropospheric zenith delay estimates, revealing an insidious pathway by which local obstructions can be misinterpreted. Collectively, these findings establish diffraction as a primary error source for high precision geodesy. It remains to be inspected however, if diffracting signals in a certain pattern based on Fresnel zone interaction, could also prove to be advantageous at the GNSS wavelength.

Future research should focus on developing real-time mitigation strategies using SNR-based detection and azimuth-dependent elevation masks, exploiting multi-frequency and multi-GNSS observations to design diffraction-resilient observables or diagnostic tools. Finally, re-analyzing long-term coordinate time series from permanent CORS stations for unrecognized diffraction effects, particularly from growing trees or new construction, may resolve some unexplained seasonal or interannual variability in current geodetic products.

References

[1] R. Emardson, P. Jarlemark, S. Bergstrand, T. Nilsson, and J. Johansson, "Measurement accuracy in network-rtk," *SP Sweden Technical Research Institute and Chalmers University of Technology. SP report*, vol. 23, 2009.

[2] A. J. Van Dierendonck, S. S. Russell, E. R. Kopitzke, and M. Birnbaum, "The GPS Navigation Message," *NAVIGATION*, vol. 25, no. 2, pp. 147–165, 1978.

[3] P. Misra and P. Enge, "Global Positioning System," *Ganga – Jamuna Press, Massachusetts, USA*, 2001.

[4] B. Hoffman-Wellenhof, H. Lichtenegger, and J. Collins, *GPS: Theory and practice*. New York: Springer Verlag, 1994.

[5] U. Dutta, J. Johansson, and R. Haas, "Investigating the impact of diffraction on GNSS carrier phase measurements," *Journal of Geodesy*, vol. 100, no. 25, 2026.

[6] K. Yedukondalu, A. Sarma, and A. Kumar, "Mitigation of gps multipath error using recursive least squares adaptive filtering," in *2010 IEEE Asia Pacific Conference on Circuits and Systems*, 2010, pp. 104–107.

[7] M. S. Braasch, "Isolation of GPS multipath and receiver tracking errors," *Journal of the Institute Navigation*, vol. 41, pp. 415–434, 1995.

[8] E. D. Kaplan and C. J. Hegarty, *Understanding GPS/GNSS - Principles and Applications*, 3rd. Artech House, 2017, ISBN: 978-1-63081-058-0.

[9] L. Wanninger and M. May, "Carrier-phase multipath calibration of GPS reference stations," in *Proceedings of the 13th International Technical Meeting of the Satellite Division of The Institute of Navigation (ION GPS-2000)*, Salt Lake City, UT, Sep. 2000, pp. 1463–1470.

[10] B. Townsend, P. C. Fenton, K. J. Van Dierendonck, and R. D. J. van Nee, “Performance evaluation of the multipath estimating delay lock loop,” in *Proceedings of The Institute of Navigation ION GPS-94*, Salt Lake City, UT, Sep. 1994.

[11] L. R. Weill, “Multipath mitigation using modernized gps signals: How good can it get?” In *Proceedings of the Institute of Navigation ION-GPS-2002*, Portland, OR, Sep. 2002, pp. 24–27.

[12] T. Rappaport, *Wireless Communications: Principles and Practice*, 2nd. USA: Prentice Hall PTR, 2001, ISBN: 0130422320.

[13] L. T. Hsu, “Analysis and modeling GPS NLOS effect in highly urbanized area,” *GPS Solutions*, vol. 22, no. 1, p. 7, 2018.

[14] J. Bradbury, *Prediction of urban GNSS availability and signal degradation using virtual reality city models*, Proceedings of the 20th International Technical Meeting of the Satellite Division of The Institute of Navigation (ION GNSS 2007), Fort Worth, TX, September 2007, pp. 2696-2706, 2007.

[15] Z. Jiang and P. D. Groves, “Nlos gps signal detection using a dual-polarisation antenna,” *GPS Solut.*, vol. 18, no. 1, pp. 15–26, Jan. 2014, ISSN: 1080-5370.

[16] P. D. Groves and Z. Jiang, “Height aiding, C/N0 weighting and consistency checking for GNSS NLOS and multipath mitigation in urban areas,” *Journal of Navigation*, vol. 66, no. 5, pp. 653–669, 2013.

[17] G. A. McGraw, P. D. Groves, and B. W. Ashman, *Robust positioning in the presence of multipath and NLOS GNSS signals*, 2020.

[18] B. Breitsch, Y. T. Morton, C. Rino, and D. Xu, “GNSS carrier phase cycle slips due to diffractive ionosphere scintillation: Simulation and characterization,” *IEEE Transactions on Aerospace and Electronic Systems*, vol. 56, no. 5, pp. 3632–3644, 2020.

[19] A. Schaper, F. Ruwisch, and S. Schön, “Diffraction modeling for improved 3DMA GNSS urban navigation,” English, in *35th International Technical Meeting of the Satellite Division of the Institute of Navigation, ION GNSS + 2022*, 2022, pp. 1902–1916.

[20] R. Xi et al., “Elimination of GNSS carrier phase diffraction error using an obstruction adaptive elevation masks determination method in a harsh observing environment,” *GPS Solutions*, vol. 27, no. 3, p. 139, Jun. 2023, ISSN: 1521-1886.

[21] R. Xi et al., "Numerical modeling and analysis of GNSS carrier-phase diffraction error in occlusion environments," *Journal of Geodesy*, vol. 99, no. 4, p. 32, Apr. 2025, ISSN: 1432-1394.

[22] U. Dutta and J. Johansson, "Multi-Constellation/Multi-Frequency GNSS Signal Degradation Due to Foliage and Reflective Environments," *Engineering Proceedings*, vol. 54, no. 1, 2023, ISSN: 2673-4591.

[23] W. Bertiger et al., "GipsyX/RTGx, a new tool set for space geodetic operations and research," *Advances in Space Research*, vol. 66, no. 3, pp. 469–489, 2020, ISSN: 0273-1177.

[24] R. Dach et al., *Bernese GNSS software version 5.2*, Nov. 2015.

[25] International GNSS Service, *Official website.*

[26] International Earth Rotation and Reference Systems Service, *Official website.*

[27] Petit, G. and Luzum, B. (eds.), "IERS Conventions," International Earth Rotation and Reference Systems Service (IERS), Frankfurt am Main, Germany, IERS Technical Note 36, 2010, p. 179.

[28] B. Hofmann-Wellenhof, H. Lichtenegger, and E. Wasle, *GNSS – Global Navigation Satellite Systems: GPS, GLONASS, Galileo, and more.* Vienna, Austria: Springer, 2008, ISBN: 978-3-211-73012-6.